



DNA Binding/Cleavage Activity, Cytotoxic, and Density Functional Theory Studies of Pyridyl-Tetrazole Cu(II) Complexes

C. Amaravathi, Shaik Mustafa, M. S. Surendra Babu*

Department of Chemistry, GITAM University Hyderabad Campus, Hyderabad - 502 329, Telangana, India.

Received 12st September 2016; Revised 09th October 2016; Accepted 11th October 2016

ABSTRACT

A new series of Cu(II) complexes were synthesized from isomeric pyridyl-tetrazole ligands such as 2-(1-vinyl-1H-tetrazol-5-yl)pyridine (L1), 2-(2-vinyl-2H-tetrazol-5-yl)pyridine (L2), N,N-dimethyl-3-(5-(pyridin-2-yl)-1H-tetrazol-1-yl)propan-1-amine(L3), and N,N-dimethyl-3-(5-(pyridin-2-yl)-2H-tetrazol-2-yl)propan-1-amine (L4). All these complexes were characterized by the elemental analysis, molar conductance, Fourier transform infrared, ultraviolet-visible (UV-VIS), magnetic moment, and electron spin resonance studies. The conductance and spectroscopic data suggested that the ligands act as monobasic bidentate ligands and form square planar complexes with general formula $[Cu(L)Cl_2]$. Highest occupied molecular orbital and lowest unoccupied molecular orbital studies of complexes were carried by density functional theory calculation using B3LYP method. Binding studies were carried by UV-VIS absorption revealed that each of these complexes is avid binders of calf thymus DNA. The nucleolytic cleavage activities of complexes were carried on double-stranded pBR322 circular plasmid DNA using a gel electrophoresis experiment under various conditions, where cleavage of DNA takes place by oxidative free radical mechanism ($\bullet OH$). Further modification of complex structure can further improve the cleavage activity in nano concentration to decrease the side effects.

Key words: Pyridyl-tetrazole, Pendant arm, Copper complexes, DNA binding.

1. INTRODUCTION

A vital polyazole heterocyclic compound is tetrazole, which can act as isostere to carboxylic group [1-4]. The major metal coordination studies are limited to metal-organic frameworks (MOF), where a tetrazole ligand is able to show nine different types of coordination, with a vast array of structural diversities having various topologies. These are used in various applications such as fluorescent sensor [5,6], organometallic, coordination chemistry [7], and organocatalysis and medicinal chemistry [8]. Copper-tetrazolate complexes have come to dominate the area of generation MOF in past few years [9-13]. Most of these synthesized frameworks or mononuclear compounds have shown interesting magnetic [8,14] catalytic [10], photoluminescence [13], or gas absorption [15] properties.

Transition metal complexes of tetrazolate have shown selective groove binding and inhibit selective cancer cells [16]. The interactions between DNA and copper tetrazolate complexes are relatively rare in the literature [17]. The DNA binding studies with tetrazolate complexes have drawn its attention

because of their site-specific binding properties. In light of the above and in continuation of our ongoing research work [18,19] on metal-DNA interactions and cytotoxic activity here, we describe the synthesis characterization, DNA binding, cleavage, and cytotoxic activity of Cu(II) complexes with regioisomeric ligands of 2-(1-vinyl-1H-tetrazol-5-yl)pyridine[L1;L2] and 2-[5-(pyridin-2-yl)-tetrazol-1-yl]propyl-N,N-dimethylamine[L3;L4].

2. EXPERIMENTAL

2.1. Materials and Reagents

Chemicals were purchased from Sigma-Aldrich and copper chloride used in the preparation of the complexes is of reagent grade. The solvents used in the synthesis of the ligands and metal complexes were distilled before use. All other chemicals were of AR grade and were used without further purification. Agarose, used in gel electrophoresis, was purchased from Sigma-Aldrich; Calf thymus (CT) DNA and plasmid pBR322 were purchased from Genie Biolabs, Bengaluru, India. The elemental analysis of carbon, hydrogen, and nitrogen contents was performed using PerkinElmer CHNS analyzer. Molar conductance

*Corresponding Author:

E-mail: manabolu@gmail.com

of the complexes was measured using a Digisun conductivity meter in dimethylformamide (DMF). The electronic absorption spectra of the complexes were recorded on a JASCO V-670 spectrophotometer in the wavelength region of 250-1400 nm. The Fourier transform infrared (FTIR) spectra of the complexes were recorded on a Tensor 2 FTIR spectrophotometer in the region of 4000-400 cm^{-1} using KBr disc.

2.2. Synthesized and Characterization of Copper Complexes

Ligands (L1-L4) were synthesis as per our previous paper [18]. The appropriate ligands (1.36 mmol) were dissolved in methanol (30 mol) and added to a $\text{CuCl}_2 \cdot \text{H}_2\text{O}$ (1.36 mmol) in methanol solution (10 mol). The resulting green-colored solutions were then heated to reflux for 2-3 h; the solution was left overnight at room temperature and filtered to collect the respective precipitate.

$[\text{Cu}(\text{L1})]\text{Cl}_2$: Dark green solid (0.14 g, yield 32%). Calculated for $\text{C}_{11}\text{H}_{16}\text{Cl}_2\text{CuN}_6$ (366.74): 36.03% (C); 4.40% (H), 22.92 % (N), found: 35.95% (C); 4.38% (H); 22.86% (N).

$[\text{Cu}(\text{L3})]\text{Cl}_2$: Dark green solid (0.11 g, yield 26%). Calculated for $\text{C}_8\text{H}_7\text{Cl}_2\text{CuN}_5$ (307.63): 31.23% (C); 2.29% (H); 22.77% (N), found: 30.95% (C); 2.18% (H); 22.76% (N).

2.3. DNA Binding and Cleavage Experiments

All measurements with CT-DNA were performed in buffer Tris-HCl 5 mM (pH 7.2), 50 mM NaCl. The ultraviolet (UV) absorbance ratio 260/280 was 1.8-1.9, indicating the DNA was sufficiently free of protein. The concentration of CT DNA per nucleotide was determined from the absorption intensity at 260 nm with the known value of $6600 \text{ M}^{-1} \text{ cm}^{-1}$. The absorption titrations were performed by adding increasing amounts of CT DNA to a solution of the complex at a fixed concentration contained in a quartz cell and recording the UV-Visible (UV-VIS) spectrum after each addition. The absorption of CT DNA was subtracted by adding the same amount of DNA to a blank. The data were then fitted to Equation (1) to obtain the intrinsic binding constant, K_b .

$$[\text{DNA}]/(\varepsilon_a - \varepsilon_f) = [\text{DNA}]/(\varepsilon_b - \varepsilon_f) + 1/K_b(\varepsilon_b - \varepsilon_f)$$

Where, [DNA] is the molar concentration of CT-DNA, ε_a , ε_b , and ε_f are apparent, free and bound metal complex extinction coefficients, respectively. Thus, K_b is the ratio of the slope to the y-intercept.

A DMF solution containing the metal complexes (250 μM) in a clean Eppendorf tube was treated with pBR322 plasmid DNA (3.3 μl of 150 $\mu\text{g}/\text{mL}$) in Tris-HCl buffer (0.10 M, pH 8.0) containing NaCl (50 mM) in presence and absence of additives. The

contents were incubated for 1 h at 37°C and loaded onto a 1% agarose gel after mixing 5 μl of loading buffer (0.25% bromophenol blue + 25% xylene cyanol + 30% glycerol, sterilized). The electrophoresis was performed at a constant voltage (80 V) until the bromophenol blue had traveled through 75% of the gel. Subsequently, the gel was stained for 10 min by immersion in ethidium bromide solution. The gel was then distained for 10 min by keeping it in sterile distilled water. The plasmid bands were visualized by viewing the gel under a transilluminator and photographed. A control experiment was done in presences of hydroxyl radical scavenger dimethyl sulfoxide (DMSO), ethylenediaminetetraacetic acid, dithiothreitol, and singlet oxygen quencher azide ion (NaN_3).

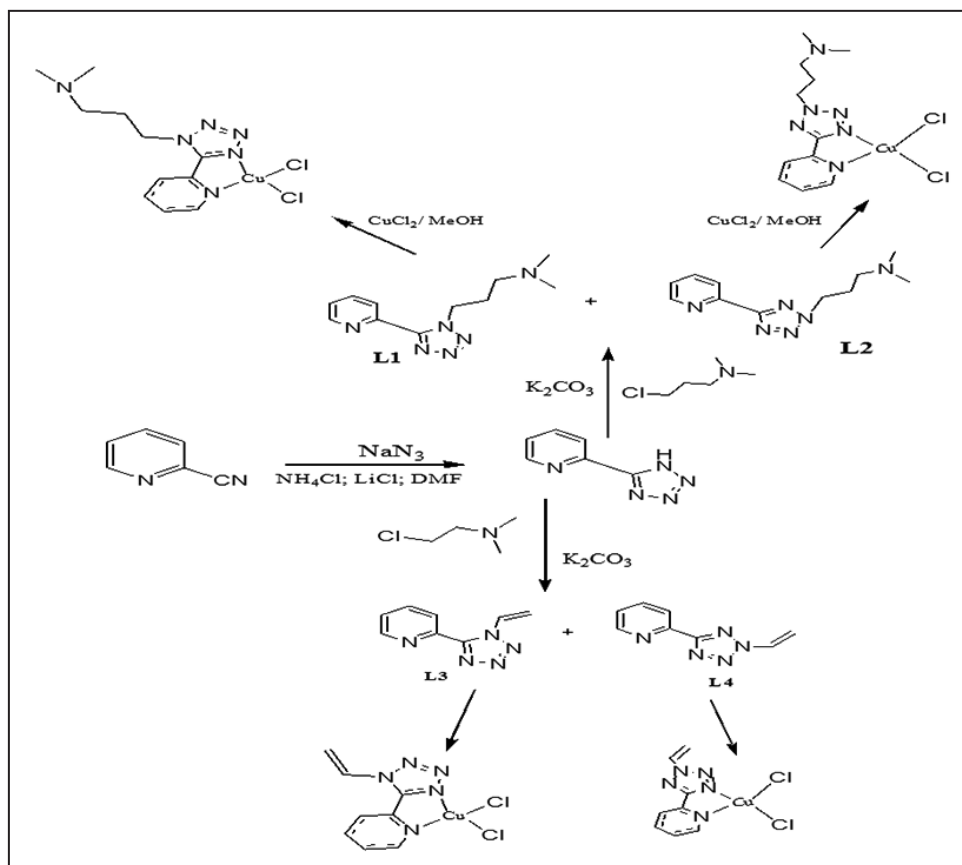
3. RESULTS AND DISCUSSION

The regioisomers L1 (2-[5-(pyridin-2-yl)-1H-tetrazol-1-yl]propyl-N,N-dimethylamine), L2 (2-[5-(pyridin-2-yl)-2H-tetrazol-2-yl]propyl-N,N-dimethylamine), and L3 (2-(1-Vinyl-1H-tetrazol-5-yl)-pyridine); L4 (2-(2-Vinyl-2H-tetrazol-5-yl)-pyridine) were prepared as per our previous paper [19] and shown in Scheme 1.

The ligands L1-L4 were treated with $\text{CuCl}_2 \cdot 2\text{H}_2\text{O}$, in refluxing methanol using a 1:1 meta/ligand ratio to give the corresponding complexes $[\text{Cu}(\text{L})\text{Cl}_2]$. The physical properties of the complexes are given in Table 1. All complexes were freely soluble in DMF, DMSO and partially in methanol and ethanol. The elemental analysis data and molar conductivity of metal complexes are in the range $135\text{-}160 \Omega^{-1} \text{ cm}^2 \text{ mol}^{-1}$ suggests that copper complexes are in 1:1 compositions. The magnetic moment values of copper complexes are in the range $1.85\text{-}2.05 \mu$, which is slightly higher than the spin-only values (1.73μ) expected for a d9 Cu(II) system [20,21].

The electronic absorption spectral data with the molar extinction coefficient of the copper complexes recorded in DMF are shown in Table 2. Electronic spectra of copper complexes (1-4) showed bands in the region 425-434 nm with high molar extinction coefficient in range $9850\text{-}7950 \text{ M}^{-1} \text{ cm}^{-1}$, which are assigned to the metal to ligand charge transfer transition ($n\text{-}\pi^*$). While single broadband observed in the region, 625-640 nm is assigned to d-d transition. The electronic spectra of these complexes display weak d-d bands in the low intensity with molar extinction coefficient $220\text{-}110 \text{ M}^{-1} \text{ cm}^{-1}$ region are assigned to ${}^2\text{E}_g \longrightarrow {}^2\text{T}_{2g}$ electronic transition; these assignments suggest a square planar geometry for the Cu(II) complexes [22].

IR spectra of L1 and L2 ligand show peaks at 2945, 1584, and 1420 cm^{-1} for L1, and at 2885, 1575, and 1415 cm^{-1} for L2 corresponding to methylene and



Scheme 1: Synthesis of ligands and copper complexes.

Table 1: Physical properties of copper complexes.

Complex	Color	Melting point °C	μ_{eff} (BM)
Cu(L1)Cl ₂	Green	172-174	1.85
Cu(L2)Cl ₂	Green	168-170	1.92
Cu(L3)Cl ₂	Dark green	136-138	1.82
Cu(L4)Cl ₂	Dark green	130-132	2.02

Table 2: Electronic spectral data λ_{max} (nm), (ϵ_{max} [M⁻¹ cm⁻¹]) of the Cu (II) complexes..

Complexes	MLCT	d-d (cm ⁻¹)
1	425 (8350)	620 (220)
2	415 (7950)	625 (210)
3	434 (9850)	640 (140)
4	430 (8740)	635 (110)

MLCT=Metal-to-ligand charge transfer

tetrazole ring; these peaks are shifted to lower frequency in all metal complexes suggesting the tetrazole group is in coordination with metal. Additional bands observed (260-220, 245-230 cm⁻¹) in the IR spectra of the metal complexes are presumably due to coordination with metal via nitrogen donor atoms.

The solid state EPR spectra of Cu(II) complexes 1 and 3 were recorded in the X-band region at room temperature (25°C), and the data are summarized in Table 3. Complex 1 and 3 exhibit g_{\parallel} values of 2.16 and 2.18 and g_{\perp} values of 2.05 and 2.06, respectively. From the observed values of complexes 1 and 3, it is clear that $g_{\parallel} > g_{\perp} > 2.00$ which suggest the fact that the unpaired electron lies predominantly in the $d_{x^2-y^2}$ orbital; characteristic of square planar geometry in Cu(II) complexes.

The geometric parameter G, which is a measure of the exchange interaction between the copper centers in the polycrystalline compound, was calculated using the Equation 1.

$$G = (g_{\parallel} - 2.0023)/(g_{\perp} - 2.0023) \quad (1)$$

According to Hathaway and Tomlinson [23], if $G > 4.0$, considerable exchange interaction is negligible because the local tetragonal axes are aligned parallel or slightly misaligned. If $G < 4.0$, exchange is considerable and the local tetragonal axes are misaligned. The observed G values of complexes are < 4.0 (Table 3 and Figure 1) suggest that there is no exchange interaction in the Cu(II) complexes.

3.1. Computational Studies

Geometry optimization of 1 and 3 complexes were carried out using density functional theory (DFT) at the B3LYP level in their ground state. The frontier orbitals of highest occupied molecular orbital (HOMO) and lowest unoccupied molecular orbital (LUMO) of Cu complex (1) are also given in Figure 2.

Thus, it is apparent that electron density of HOMO in Cu(II) complexes have largely localized on pyridine ring and partly on tetrazole ring but in LUMO electrons are largely localized on tetrazole ring. The HOMO-LUMO energy gap in the ground state of complex 1 and complex 3 has been predicted to be 0.35272 and 0.25326 eV, respectively, and is not influenced by excitation. From the optimized structure of complex 1, the bond lengths of Cu-Cl atoms are 2.32 Å and 2.33 Å and bond angle Cl-Cu-Cl of 31.5 Å, whereas

Table 3: ESR spectral assignments for complexes 1 and 3 at room temperature.

Complexes	g_{\parallel}	g_{\perp}	g_{av}	G
1	2.16	2.05	2.102	3.306
3	2.18	2.06	2.117	3.079

ESR=Electron spin resonance

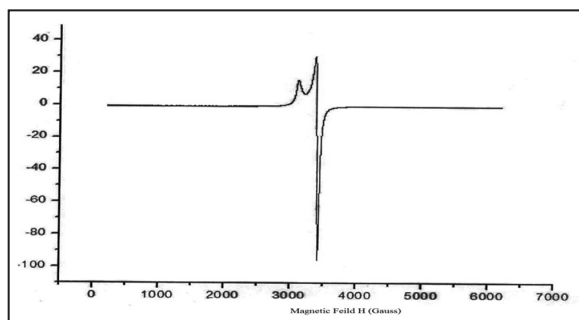


Figure 1: X-band electron spin resonance spectra of the complex 1 at room temperature.

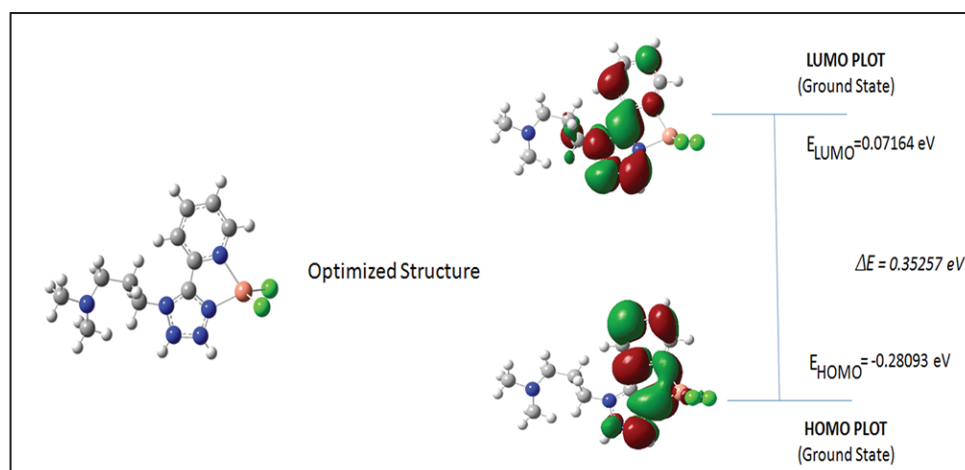


Figure 2: The optimized structure, highest occupied molecular orbital, and lowest unoccupied molecular orbital of complex 1.

vinyl copper complex (3) the bond lengths of Cu-Cl atoms are 2.16 Å and bond angle Cl-Cu-Cl of 45 Å, respectively.

3.2. DNA Binding Activity

The binding interactions of 1-4 complexes with CT-DNA were monitored by UV-VIS spectroscopy. The complexes were stable in Tris buffer solutions [24]. The absorption spectra of the copper complexes are compared with and without CT DNA at 400-500 nm range. Electronic absorption spectral data upon addition of CT-DNA and binding constants of these complexes are given in Table 4. Typical absorption spectrum of complex 1 is shown in Figure 3. In the presence of increasing amounts of CT-DNA, the UV-VIS absorption spectra of complexes 1-4 showed increase in absorbance exhibiting bathochromic shift (0.5-2.5 nm) with hyperchromism (2.5-11.4%) with respect to control (0 μl DNA). The change in absorbance values with increasing amount of CT-DNA was used to evaluate the intrinsic binding constant K_b (Table 4).

It is evident from the Table 4 that all the complexes bind with DNA with high affinities and, the estimated binding constants are in the range $4.0-6.2 \times 10^4 M^{-1}$. The K_b values of 1-4 complexes are comparable with the reported values for redox active complexes. The intrinsic binding constant for cisplatin, which shows a hyperchromic shift after subsequent addition of CT-DNA is reported as $3.20 \times 10^4 M^{-1}$ [25].

The binding nature of present complexes is significant due to π -stacking interaction of planar pyridyl-tetrazole rings. Binding of complexes to CT-DNA by external contact (electrostatic or groove binding) brings about bath chromic shift with hyperchromism absorption intensity [26]. A strong binding constant for 1, may be attributed to greater symmetric nature and electrostatical interaction ($-N(CH_3)_2$) with CT.

3.3. DNA Cleavage Activity

The nuclease activity of metal complexes has been investigated on supercoiled plasmid DNA pBR322 by agarose gel electrophoresis in the absence and

presence of oxidant (H_2O_2) at 120 min incubation period. The gel electrophoresis diagram is shown in Figure 4. In Figure 4, all even numbered lanes are run in the presence of oxidant and all odd lanes in the absence of oxidant (H_2O_2). The gel mainly contains complex 1 in lane 5 and 6, complex 2 in lane 7 and 8, complex 3 in lane 9 and 10, and complex 4 in lane 11 and 12, respectively. All pyridyl-tetrazole complexes have shown a significant cleavage activity in micromolar concentration for 2 h incubation period, in the absence and presence of oxidant (H_2O_2) at the physiological temperature and pH (7.2). The nuclease activity is greatly enhanced by conversion of Form I to Form II and Form III on incorporation of copper ion in the pyridyl-tetrazole ligands. While in lanes 9-12 containing complex 3

Table 4: Effect of CT DNA on the absorbance bands and binding constant of the copper complexes.

Complexes	λ_{max} (nm)		$\Delta\lambda$ (nm)	H (%)	K_b (M^{-1})
	Free	Bound			
I	433.5	431.0	2.5	7.4	4.5×10^4
II	443.0	442.5	0.5	6.5	3.5×10^4
III	344.5	343.5	1.0	4.5	2.3×10^4
IV	344.0	343.5	0.5	2.5	2.1×10^4

CT=Calf thymus

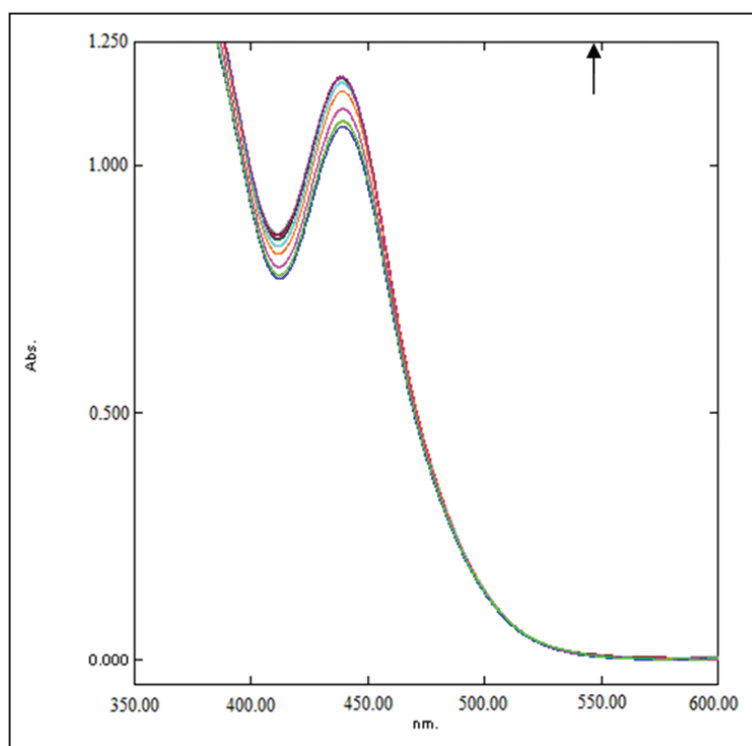


Figure 3: Effect of calf thymus DNA on the absorbance bands and binding constant of complex (2) and adducts.

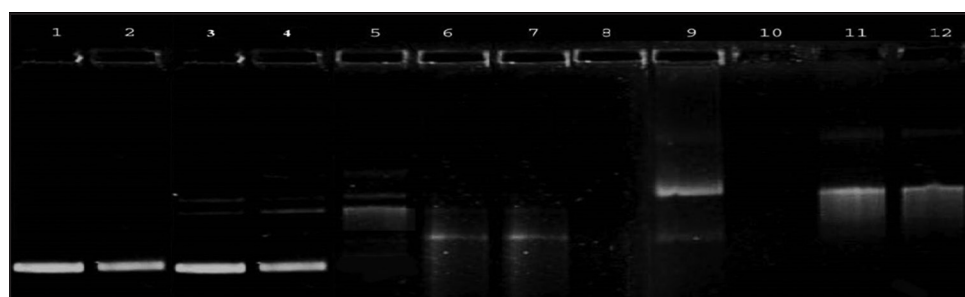


Figure 4: Agarose gel (1%) showing the results of electrophoresis of 1 ml of pBR322 plasmid DNA ($0.10 \mu g ml^{-1}$) and 2 ml of 0.1 M Tris-HCl buffer (pH 8.0): 70.5 mM complex in dimethylformamide; 10 mM H_2O_2 were added, respectively, incubation at 37°C (120 min). Lane 1: DNA (control); Lane 2: DNA+ H_2O_2 (control); Lane 3: DNA+1; Lane 4: DNA+1+ H_2O_2 ; Lane 5: DNA+2; Lane 6: DNA+2+ H_2O_2 ; Lane 7: DNA+3; Lane 8: DNA+3+ H_2O_2 ; Lane 9: DNA+4; Lane 10: DNA+4+ H_2O_2 .

and 4 in presence and absences of H₂O₂, Form I is completely converted Form II and Form III and with formation of smears [27].

4. CONCLUSIONS

Pyridyl-tetrazole pendent arm containing -vinyl and -propyl-dimethylamine, mononuclear Cu(II) complexes of novel bidentate ligands have been synthesized and characterized. Physicochemical and spectral studies reveal that mononuclear complexes have distorted square planar geometry. Complex 1 show higher binding constant (K_b) with CT-DNA may be due to more symmetric nature. In the presence of H₂O₂, complexes cleave DNA more efficiently which may be due to the reaction of hydroxyl radical with DNA. All the complexes cleave DNA via oxidative path. DNA cleavage and binding activity of present complexes is good and encourages designing better and efficient metal-based drugs.

5. REFERENCES

1. M. Wriedt, J. P. Sculley, A. A. Yakovenko, Y. Ma, G. J. Halder, P. B. Balbuena, H. C. Zhou, (2012) Low-energy selective capture of carbon dioxide by a pre-designed elastic single-molecule trap, *Angewandte Chemistry International Edition*, **51**: 9804.
2. Y. Qiu, B. Liu, G. Peng, J. Cai, H. Deng, M. Zeller, (2010) Construction of two mercury(II) coordination frameworks involving *in situ* tetrazole ligand synthesis, *Inorganic Chemistry Communications*, **13**: 749.
3. R. J. Herr, (2002) 5-Substituted-1H-tetrazoles as carboxylic acid isosteres: Medicinal chemistry and synthetic methods, *Bioorganic and Medicinal Chemistry*, **10**: 3379.
4. M. Ahmad, M. Y. Wani, S. A. Al-Thabaiti, R. A. Shiekh, (2014) Gamma-cyclodextrin on enhancement of water solubility and store stability of nystatin, *Journal Including Phenom Macrocyclic Chemistry*, **78**: 15.
5. Y. Zhang, X. Guo, L. Jia, S. Xu, Z. Xu, L. Zheng, X. Qian, (2012) Substituent-dependent fluorescent sensors for zinc ions based on carboxamidoquinoline, *Dalton Trans*, **41**: 11776.
6. L. Lv, M. Cao, J. Li, J. Wang, (2013) A sensitive ratiometric fluorescent sensor for zinc(II) with high selectivity, *Sensors*, **13**: 3131.
7. G. Aromi, L. A. Barrios, O. Roubeau, P. Gamez, (2011) Triazoles and tetrazoles: Prime ligands to generate remarkable coordination materials, *Coordination Chemistry Reviews*, **255**: 485.
8. M. Y. Wani, A. R. Bhat, A. Azam, I. Choi, F. Athar, (2012) Probing the antiameobic and cytotoxicity potency of novel tetrazole and triazine derivatives, *European Journal of Medicinal Chemistry*, **48**: 313.
9. Z. J. Hou, Z. Y. Liu, N. Liu, E. C. Yang, X. J. Zhao, (2015) Four tetrazolate-based 3D frameworks with diverse subunits directed by inorganic anions and azido coligand: Hydro/solvothermal syntheses, crystal structures, and magnetic properties, *Dalton Transactions*, **44**: 2223.
10. R. Nasani, M. Saha, S. M. Mobin, L. M. D. Martins, A. J. L. Pombeiro, A. M. Kirillov, S. Mukhopadhyay, (2014) Copper-organic frameworks assembled from *in situ* generated 5-(4-pyridyl) tetrazole building blocks: Synthesis, structural features, topological analysis and catalytic oxidation of alcohols, *Dalton Transactions*, **43**: 9944.
11. T. Pham, K. A. Forrest, A. Hogan, K. McLaughlin, J. L. Belof, J. Eckert, B. Space, (2014) Simulations of hydrogen sorption in rht-MOF-1: Identifying the binding sites through explicit polarization and quantum rotation calculations, *Journal of Materials Chemistry A*, **2**: 2088.
12. Y. Kim, S. Huh, (2016) Pore engineering of metal-organic frameworks: Introduction of chemically accessible Lewis basic sites inside MOF channels, *Crystal Engineering Communication*, **18**: 3524.
13. L. Bergmann, J. Friedrichs, M. Mydlak, T. Baumann, M. Nieger, S. Bräse, (2013) Outstanding luminescence from neutral copper(I) complexes with pyridyl-tetrazolate and phosphine ligands, *Chemistry Communications*, **49**: 6501.
14. X. M. Zhang, J. Lv, F. Ji, H. S. Wu, H. Jiao, P. V. R. Schleyer, (2011) A perfectly square-planar tetracoordinated oxygen in a tetracopper cluster-based coordination polymer, *Journal of the American Chemical Society*, **133**: 4788.
15. P. Pachfule, Y. Chen, S. C. Sahoo, J. Jiang, R. Banerjee, (2011) Structural isomerism and effect of fluorination on gas adsorption in copper-tetrazolate based metal organic frameworks, *Chemistry of Materials*, **23**: 2908.
16. A. Haleel, P. Arthi, N. D. Reddy, V. Veena, N. Sakthivel, Y. Arun, P. T. Perumald, A. K. Rahiman, (2014) DNA binding, molecular docking and apoptotic inducing activity of nickel(II), copper(II) and zinc(II) complexes of pyridine-based tetrazolo[1,5-a]pyrimidine ligands, *RSC Advances*, **4**: 60816.
17. M. Saha, M. Das, R. Nasani, I. Choudhuri, M. Yousufuddin, H. P. Nayek, M. M. Shaikh, B. Pathak, S. Mukhopadhyay, (2015) Targeted water soluble copper-tetrazolate complexes: Interactions with biomolecules and catecholase like activities, *Dalton Transactions*, **44**: 20154.
18. S. Mustafa, B. U. Rao, M. S. S. Babu, K. K. Raju, G. N. Rao, (2015) Synthesis, characterization, and biological activities of pendant arm-pyridyltetrazole copper(II) complexes: DNA binding/cleavage activity and cytotoxic studies, *Chemistry and Biodiversity*, **12**: 1516.
19. M. S. S. Babu, B. U. Rao, V. Krishna, S. Mustafa, G. Nageswara Rao, (2015) Synthesis, characterization and DNA cleavage studies of

- isomeric pyridyl-tetrazole ligands and their Ni(II) and Zn(II) complexes, *Journal of Saudi Chemical Society*. Available from: <http://www.dx.doi.org/10.1016/j.jscs.2015.07.003>.
20. W. J. Geary, (1971) The use of conductivity measurements in organic solvents for the characterisation of coordination compounds, *Coordination Chemistry Reviews*, **7**: 81.
 21. B. J. Hathaway, (1987) In: G. Wilkinson, R. D. Gillard, J. A. McCleverty, (Eds.), *Comprehensive Coordination Chemistry*, Vol. 5. Oxford: Pergamon Press, p583.
 22. B. J. Hathaway, A. A. G. Tomlinson, (1970) Copper(II) ammonia complexes, *Coord. Chemical Reviews*, **5**: 1.
 23. J. Nagaj, S. S. Kamila, K. Ewa, F. Tomasz, J. B. Małgorzata, B. Wojciech, (2013) Revised coordination model and stability constants of Cu(II) complexes of Tris buffer, *Inorganic Chemistry*, **52**: 13927.
 24. M. Usman, F. Arjmand, M. Ahmad, M. S. Khan, I. Ahmad, S. Tabassum, (2016) Comparative analyses of bioactive Cu(II) complexes using hirshfeld surface and density functional theory (DFT) methods: DNA binding studies, Cleavage and Antibiofilm activities, *Inorganica Chimica Acta*, **453**: 193.
 25. K. Suntharalingam, O Mendoza, A. A. Duarte, D. J. Mann, R. Vilar, (2013) A platinum complex that binds non-covalently to DNA and induces cell death via a different mechanism than cisplatin, *Metallomics*, **5**: 514.
 26. R. S. Kumar, S. Arunachalam, V. S. Periasamy, C. P. Preethy, A. Riyasdeen, M. A. Akbarsha, (2008) Synthesis, DNA binding and antitumor activities of some novel polymer-cobalt(III) complexes containing 1,10-phenanthroline ligand, *Polyhedron*, **27(3)**: 1111.
 27. W. K. Pogozelski, T. D. Tullius, (1998) Oxidative strand scission of nucleic acids: Routes initiated by hydrogen abstraction from the sugar moiety, *Chemical Reviews*, **98(3)**: 1089.

***Bibliographical Sketch**



Dr. M.S. Surendra Babu had completed his M.Sc. (Organic Chemistry) M.Phil and Ph.D. in Bioinorganic Chemistry from Sri Krishnadevaraya University, India. He qualified CSIR-UGC (NET) in June - 2002. His major research area is "DNA interactions with metal complexes." After completion of Ph.D., he worked as research scientist in R&D industries for 2 years. At present, he is working as Assistant Professor, in Department of Chemistry, GITAM University, Hyderabad Campus, Hyderabad, India since 2009.